

# COMPUTATIONAL SCREENING FOR LOW EMITTANCE PHOTOCATHODES

J. T. Paul\*, R. G. Hennig, University of Florida, Gainesville, USA  
A. Galdi, I. V. Bazarov, Cornell University (CLASSE), Ithaca, USA  
S. Karkare, H. Padmore, Lawrence Berkley National Lab, Berkeley, USA

## Abstract

The majority of photocathode materials in use in accelerator applications have been discovered empirically through trial and error with little guidance from material science calculations. Alternatively, one can envision a process which is heavily guided by computational search using latest advances in density functional theory (DFT). In this work, the MaterialsProject database is searched for potential single crystal photocathodes that would be suitable for ultralow emittance beam production. The materials in the database are initially screened on the basis of experimental practicality. Following this, the expected emittance is calculated from the DFT computed band structures for the pre-screened materials using the conservation of energy and transverse momentum during photoemission. Based on such computational screening, we provide a list of potential low emittance photocathode materials which can be investigated experimentally as high brightness electron sources.

## INTRODUCTION

A great deal of progress has been made in the photocathode community through experiment-driven research. However, by complementing experimental efforts with computational approaches, the discovery and characterization of novel electron sources can be accelerated. Together, insights into the behavior of materials and what properties are required for high brightness electron emission can be made.

To perform theory-driven research on photocathodes, density functional theory (DFT) provides an ideal combination of good accuracy and sufficiently low computational cost. DFT solves the set Kohn-Sham equations to determine the ground state electron density and energy of a material [1, 2], which in turn can be used to provide various materials properties, such as atomic structure, band gap, effective masses, surface states, and quantum efficiency.

The aim of this work is to identify potential innovative photocathode materials, based on DFT evaluation of quantum efficiency (QE) and intrinsic emittance that we quantify in terms of mean transverse energy (MTE) of the photoelectrons. High brightness photocathode sources have to generate electron beams with low MTE and have sufficient QE to produce electron pulses with the required charge for applications.

The materials are selected from the MaterialsProject computational materials database by using a series of screening criteria in order to limit the computational effort of the full

DFT calculations to a subset of promising candidates. The approach described in the following applies to materials with an energy gap; a different methodology will be developed for metals.

## METHODS

To begin the work, the MaterialsProject database was used as the source of crystalline compounds [3]. The materials repository contains over 69,000 crystal structures and over 53,000 electronic band structures. The database contains both experimentally synthesized compounds, i.e. the crystal structure has an associated entry in the inorganic crystal structure database (ICSD) [4], and computationally predicted phases. In this work, we include both types of compounds to ensure a thorough search. Using the Materials Application Programming Interface (MAPI), information of these crystal structures was obtained using the pymatgen software package [5]. In order to improve efficiency of the photocathode screening, several filters were applied to the MaterialsProject database.

Next, we use the Vienna Ab-initio Simulation Package (VASP) DFT package to perform the quantum mechanical calculations of the work [6]. Structures obtained from MaterialsProject are largely accepted as-is, though some materials do undergo structural optimization. The electronic band structure of each compound is calculated for each compound in order to identify the effective mass. Candidates that pass through this screening process will be turned into slabs in order to account for the surface, vacuum and time-reversed LEED-like states [7]. Finally, we plan to determine the QE using the matrix elements for the optical excitations, calculating how many electrons are excited to the vacuum compared to how many electrons are excited to states within the material and identifying the mean transverse energy (MTE) of a particular crystal face.

## RESULTS

To begin the screening of the MaterialsProject database, all materials containing radioactive elements were screened out. Following, all materials with a hull distance greater than 50 meV/atom were removed from the list of potential photocathodes. The hull distance is a measure of the metastability of a material, with a distance of 0 meV/atom (i.e. on the hull) being considered the ground state. An example of a thermodynamic hull can be seen in Fig. 1. Any compound above the thermodynamic hull (the blue dots and lines) are inherently unstable since there is a more energetically favorable phase or combination of phases, which the unstable compound can

\* joshuapaul@ufl.edu

Content from this work may be used under the terms of the CC BY 3.0 licence (© 2018). Any distribution of this work must maintain attribution to the author(s), title of the work, publisher, and DOI.

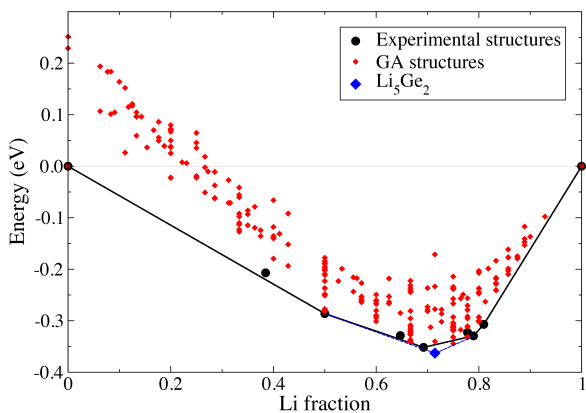


Figure 1: The thermodynamic hull of the Li-Ge binary system. Black dots indicate experimental phases while red dots represent phases identified with a genetic algorithm. The blue diamond indicates  $\text{Li}_5\text{Ge}_2$ , which falls below the previous thermodynamic hull, indicating that it is the actual ground state at its composition. Blue dashed lines represent the new convex hull resulting from the discovery of  $\text{Li}_5\text{Ge}_2$ . For more discussion on Li-Ge search, see [8]. For more discussion thermodynamic stability, see [9].

decompose into. However, either through entropic contributions to the Gibbs free energy or kinetic restrictions, bulk materials that are metastable up to about 50 meV/atom can sometimes be synthesized [9], and thus, we use this value as screening criteria for stability. Next, we removed all metals and materials with a listed band gap greater than 4 eV. Note that the PBE exchange-correlation functional [10] used to estimate the band gap in MaterialsProject is known to underestimate the band gap by up to 50% [11, 12], and thus the true cap on band gaps is closer to 6 eV. Table 1 shows that the screening by our criteria of radioactivity, stability, and bandgap reduces the number of materials from 69,640 to 38,019.

After this preliminary screening, the effective masses of the materials were calculated using the band structures calculated in the MaterialsProject database. The effective mass is proportional to the mean transverse energy of an electron, so a low effective mass indicates the material is likely to have a lower MTE since the electron has a lower transverse

Table 1: Screening Process

Screening	Number of materials
MaterialsProject Database	69,640
No Radioactive Elements	66,119
$\Delta E_{hull} \leq 50$ meV/atom	43,087
$0 \text{ eV} < E_{gap} \leq 4$ eV	38,019
20 $k$ -points: $m^* \leq .2m_0$	517
200 $k$ -points: $m^* \leq .2m_0$	In Progress
High Quantum Efficiency	In Progress
Low MTE	In Progress

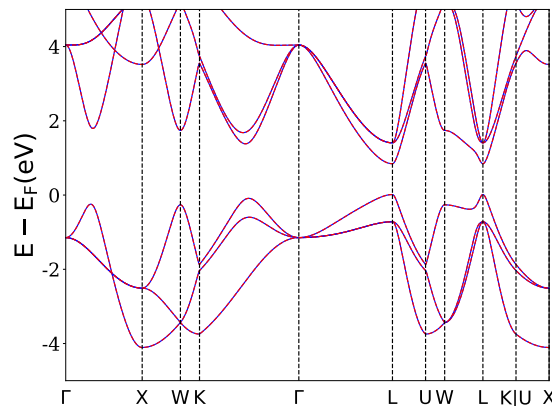


Figure 2: The electronic band structure of PbTe. Each letter represents a high symmetry point within reciprocal space. One can see high curvatures in the bands at L points, indicating a low MTE due to transverse momentum of the electron

momentum upon emission. The electronic band structure of PbTe is provided as Fig. 2 for reference. We assume that electrons may be emitted either from the Valance Band Maximum (VBM) or from the Conduction Band Minimum (CBM) and hence calculated the effective masses of both the VBM and CBM. Electrons can be present in the CBM either by appropriate doping or via optical excitation prior to emission. The effective mass is determined by the equation

$$m^* = \frac{\hbar^2}{m_0 * d^2E/dk^2},$$

where  $m^*$  is the effective mass,  $E$  is the energy of the system,  $k$  is distance in reciprocal space, and  $m_0$  is the mass of an electron. This indicates that the effective mass is inversely proportional to the curvature of the VBM and CBM, and the electronic band structure can be used to estimate the effective mass of a photocathode candidate via a parabolic fit. However, the band structures in the MaterialsProject database are relatively coarse, with 20  $k$ -points between every high symmetry point in reciprocal space. This is typically enough for obtaining band gaps and imaging band structures, however, it results in a poor estimation of the effective mass as the relevant energy range is not well mapped. Thus, we use the effective mass of the rough band structure as a first cut-off, specifically  $m^* < 0.2m_0$ , which results in 517 potential low-emittance photocathodes. Note that the effective mass on each side of the VBM and CBM was considered, as each side represents different directions in the crystal lattice.

Next, the DFT software VASP was used to structurally reoptimize some of the compounds obtained from the MaterialsProject database. Following this, we recalculate the electronic band structure of all compounds that have survived the screening and identified how dense a  $k$ point mesh was needed in order to properly estimate the effective mass.

Using intervals of 50, 100, and 200  $k$ -points between every high symmetry point, three and six  $k$ -points were used to fit the effective mass. The results of some of this fitting can be seen in Fig. 3. As can be seen, the difference between three and five points for fitting decreases significantly as the number of  $k$ -points between every high symmetry point increases. Though there isn't a cost to increasing the number of  $k$ -points, noise eventually begins to impact the fit, resulting in poor identification of the VBM and CBM in reciprocal space as well as poor fitting for the effective mass. Thus, it was decided that 200  $k$ -points per high symmetry path was sufficient for estimating the effective mass.

Following the identification of low effective mass materials, slabs of these materials must be generated. Although the low effective mass indicates the possibility of a low MTE, various factors like the presence of surface states, non-availability of appropriate conduction band states for excitation etc. can tarnish this behavior. Alternatively, there may be features of a surface state that can be taken advantage of to improve the photocathode performance [13]. Thus, slabs of the passing photocathode candidates must be generated. When generating said slabs, two criteria must be ensured: the slab is thick enough to properly represent the bulk electronic states of the material, and the vacuum spacing is large enough to prevent the periodic image of the slab from interacting with itself. A vacuum spacing of 15 Å is typically sufficient to prevent the periodic image from interacting with itself. Slab thickness convergence is less precise, though a general estimate can be found by converging several candidate photocathodes.

Once the slab thicknesses are converged, the band structure can be calculated for the photocathode candidate slabs. By determining the decay of an orbital into the vacuum, electronic states associated with the material can be differentiated from the time-reversed LEED states (visualized in Fig. 4). Namely, the states associated with the material will not be sustained outside the material and the wave function will decay in vacuum. Vacuum states, however, will not and as a result the bands can be differentiated. VASP can

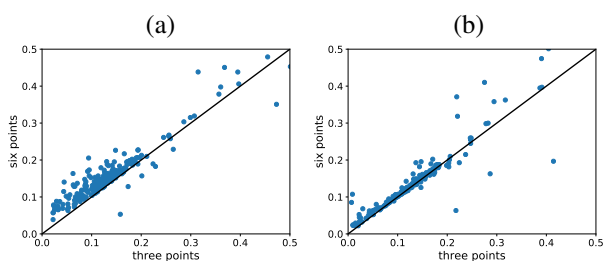


Figure 3: The effective masses of the parabolic fit with three points and six points per fit, with each dot representing a unique materials and the line representing a 1:1 ratio of the fit. (a) is the fit with a kpoint density of 50  $k$ -points per high symmetry path while (b) is the fit with 200  $k$ -points per high symmetry path. The difference in the fits drops dramatically as the number of  $k$ -points used increases.

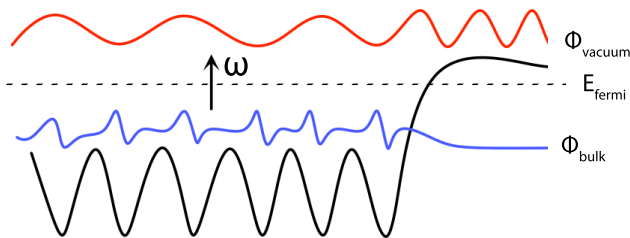


Figure 4: Examples of time-reversed LEED state that exist in vacuum. The black line represents the potential within the material while the blue line represents the initial wave function of a ground state electron within the bulk of a material. The red lines represents an electron that has been excited into vacuum. Using VASP, the ratio of electrons excited from the bulk states to these vacuum states can be determined. For further discussion on this topic, please refer to [14].

also calculate the dielectric response of a material, during with it identifies the strength of an optical transition from one band to another. By combining this information with the knowledge of which bands are associated with the bulk, the surface, and the vacuum, a relative scale of quantum efficiency can be used to rank the photocathode candidates. Finally, by combining information about the effective mass and the optical transitions, an estimate on the MTE can be made computationally. This final phase of the work is currently ongoing.

## CONCLUSIONS

Using computational databases and techniques, over 69,000 unique crystalline compounds were screened for their potential as photocathodes. Using initial criteria based on elemental composition, stability, and electronic band gap, this number was narrowed down to 38,019 compounds. The effective mass of these compounds were then roughly estimated to narrow the search to 517 compounds, which were then simulated to calculate a more accurate effective mass. This effective mass, converged with the number of  $k$ -points used in the band structure calculation, is to be used to further screen the number of photocathodes investigated. Based on this criteria, some materials such as KCdAs, Ba<sub>2</sub>BiAu, InP, and NaSbS<sub>2</sub> may have a low MTE. Following, the quantum efficiency of the photocathode candidates will be calculated through optical transition elements, allowing for an estimate of the MTE to be made and a set of candidate photocathodes to be recommended for synthesis.

## ACKNOWLEDGEMENTS

This work is supported by the National Science Foundation under grants Nos. DMR-1542776, ACI-1440546, and PHY-1549132, the Center for Bright Beams. Calculations were performed on the University of Florida HiPerGator Supercomputer.

## REFERENCES

- [1] P. Hohenberg and W. Kohn, "Inhomogeneous electron gas," *Phys. Rev.*, vol. 136, pp. B864–B871, Nov 1964.
- [2] W. Kohn and L. J. Sham, "Self-consistent equations including exchange and correlation effects," *Phys. Rev.*, vol. 140, pp. A1133–A1138, Nov 1965.
- [3] A. Jain, S. P. Ong, G. Hautier, W. Chen, W. D. Richards, S. Dacek, S. Cholia, D. Gunter, D. Skinner, G. Ceder, and K. a. Persson, "The Materials Project: A materials genome approach to accelerating materials innovation," *APL Materials*, vol. 1, no. 1, p. 011002, 2013.
- [4] A. Belsky, M. Hellenbrandt, V. L. Karen, and P. Luksch, "New developments in the Inorganic Crystal Structure Database (ICSD): accessibility in support of materials research and design," *Acta Crystallographica Section B*, vol. 58, pp. 364–369, Jun 2002.
- [5] S. P. Ong, W. D. Richards, A. Jain, G. Hautier, M. Kocher, S. Cholia, D. Gunter, V. L. Chevrier, K. A. Persson, and G. Ceder, "Python materials genomics (pymatgen): A robust, open-source python library for materials analysis," *Computational Materials Science*, vol. 68, pp. 314 – 319, 2013.
- [6] G. Kresse and J. Furthmüller, "Efficient iterative schemes for ab initio total-energy calculations using a plane-wave basis set," *Phys. Rev. B*, vol. 54, pp. 11169–11186, Oct 1996.
- [7] S. Karkare, W. Wan, J. Feng, T. C. Chiang, and H. A. Padmore, "One-step model of photoemission from single-crystal surfaces," *Phys. Rev. B*, vol. 95, p. 075439, Feb 2017.
- [8] W. W. Tipton, C. A. Matulis, and R. G. Hennig, "Ab initio prediction of the li5ge2 zintl compound," *Computational Materials Science*, vol. 93, pp. 133–136, 2014.
- [9] W. Sun, S. T. Dacek, S. P. Ong, G. Hautier, A. Jain, W. D. Richards, A. C. Gamst, K. A. Persson, and G. Ceder, "The thermodynamic scale of inorganic crystalline metastability," *Science Advances*, vol. 2, no. 11, 2016.
- [10] J. P. Perdew, K. Burke, and M. Ernzerhof, "Generalized gradient approximation made simple," *Phys. Rev. Lett.*, vol. 77, pp. 3865–3868, Oct 1996.
- [11] J. P. Perdew and M. Levy, "Physical content of the exact kohn-sham orbital energies: Band gaps and derivative discontinuities," *Phys. Rev. Lett.*, vol. 51, pp. 1884–1887, Nov 1983.
- [12] J. P. Perdew, "Density functional theory and the band gap problem," *International Journal of Quantum Chemistry*, vol. 28, no. S19, pp. 497–523, 1985.
- [13] S. Karkare, J. Feng, X. Chen, W. Wan, F. J. Palomares, T.-C. Chiang, and H. A. Padmore, "Reduction of intrinsic electron emittance from photocathodes using ordered crystalline surfaces," *Phys. Rev. Lett.*, vol. 118, p. 164802, Apr 2017.
- [14] J. Minár, "Theoretical description of arpes: The one-step model," in *DMFT at 25: Infinite Dimensions*, ch. 13, pp. 13.1–13.39, Forschungszentrum Jülich GmbH Institute for Advanced Simulation, 2014.